Object Detection of Components in a Radiograph for Treaty Verification Behind an Information Barrier

Matthew R. Marshall, Heidi Komkov, Erik Brubaker
Sandia National Laboratories[1]
Albuquerque, New Mexico, USA

Abstract
Information from an x-ray radiograph can identify the presence or absence of components within a treaty accountable item (TAI). However, the radiograph could contain sensitive information which a treaty partner does not wish to reveal. Information protection necessitates automated image processing, without the use of a human inspector, for which no widely accepted methods yet exist. This study explores deep learning-based computer vision models applied to confirming presence/absence of components in radiographs for treaty verification behind an information barrier. Unlike methods that require a reference image of the TAI, the computer vision model is trained on non-sensitive images, into which the agreed-upon component of interest is synthetically inserted. Despite training on non-sensitive backgrounds, the model is able to ultimately identify the presence/absence of the component in a sensitive context.

1) Introduction

Nuclear warhead verification could be required in a future arms control treaty. X-ray radiography is a method of visualizing the internal structure of a treaty accountable item (TAI) such as a warhead, and can enable determination of its authenticity, type, or readiness level. Treaty partners may agree to share designs of non-nuclear components that could be identified in a radiograph to enable the desired determinations. In this paper, we explore automatic item identification using computer vision in radiographs without the need for a human inspector.

Interpreting radiographs behind an information barrier is a challenging problem. Prior work in this space applied conventional image processing techniques to radiography by first performing feature detection on a test and reference image, and then comparing the features between the two images [1, 2]. While successful at verifying similarity of radiographed items behind an information barrier, this approach requires the use of a reference image for verification. A reference image can contain highly sensitive information making this approach less amenable to implementation. Furthermore, today's state-of-the-art deep learning-based computer vision methods generally outperform conventional image processing techniques for feature extraction and object detection.

In this work, we use a non-sensitive analog scenario involving automotive engines to demonstrate how a computer vision model trained on non-sensitive radiographs and an agreed-upon design component of a TAI from treaty negotiations can be used to identify that design component in a different context, within the TAI. As an example design component, we use an engine piston. For non-sensitive backgrounds, we use radiographs of pelican briefcases filled with everyday items, multiplicatively inserting the piston into the images to create an annotated training set for object detection. The sensitive context, forming the test set, is the piston (one or multiple) inside of an engine. All radiographs are simulations generated from CAD models.

[1]Sandia National Laboratories is a multimission laboratory managed and operated by National Technology and Engineering Solutions of Sandia, LLC, a wholly owned subsidiary of Honeywell International Inc., for the U.S. Department of Energy's National Nuclear Security Administration under contract DE-NA0003525.

2) Methods

a) X-ray Interactions with Materials

X-ray intensity (ϕ) decreases exponentially as an x-ray passes through a material with attenutation coefficient μ and thickness d (ignoring energy-dependent effects):

$$\phi_f = \phi_i e^{-\mu d}. \quad (1)$$

To model all interactions of an x-ray passing through n materials, we can apply a summation to the exponential term in Equation 1:

$$\phi_f = \phi_i e^{-\sum_{j=1}^{n} \mu_j d_j}. \quad (2)$$

b) Synthetic Data Generation

To generate synthetic x-ray radiographs from CAD models, we use the Radiation Training Simulator plug-in within X-Ray ToolKit (XTK) Software [3], a Sandia National Laboratories (SNL) developed program. The Radiation Training Simulation is a first-order approximation that generates synthetic radiographs using raytracing. At a high level, the program draws a line from an x-ray generator to a pixel on an imager plate, and computes the attenuation (Equation 2) as a result of the x-ray interaction with the materials in the line's path. This process is repeated for every pixel on the imager plate.

To improve realism, 5 mm of jitter is applied to the ray's starting point. A Gaussian blur with a radius of 5 pixels is applied at the end of the computation to smooth out jagged edge artifacts that are a result of only computing one ray per pixel. The simulation does not account for pair production, scattering, or other physical effects. In comparison to real radiographs, there are fewer artifacts and less image-to-image variation. The raytracing approach enables the quick generation of synthetic radiographs, on the order of seconds to minutes per image.

c) Analog Problem Setup

As a non-sensitive analog scenario, we use a car engine as a treaty accountable item, with a piston being the design component of interest. Figure 1 shows the CAD model of the car engine (left pane) and a radiograph of it (right pane) using XTK, with 6000 keV X-rays and a pulse time of 30 seconds. The lines in the radiograph are the divisions between the multiple x-ray detector panels that would be necessary to image the whole engine. We test on only single panels.

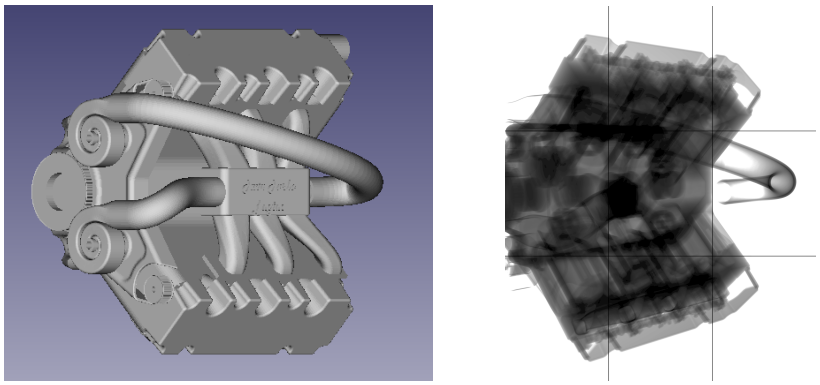

Figure 1 – The analog treaty accountable item used in this study, an automotive engine. The design component of interest is a piston. On the left is a CAD model of the engine, and on the right is a simulated radiograph of it using XTK.

To train a computer vision model, a large amount of training data is needed. We generate 3072 unique views of the piston from evenly spaced locations around a sphere. For training, we use 250 randomly composed backgrounds of pelican cases containing everyday items, into which we insert the piston images as described in the next section, to create a total of 12000 training images and 400 validation images. The pelican cases contain water bottles, springs, hammers, wrenches, aluminum plates, and steel pipes, and they are imaged using the same simulation settings as the engines. For testing, we use 48 single-panel views of the engine, of which 15 examples were negatives. Figure 2 shows examples of the piston, training, and testing images.

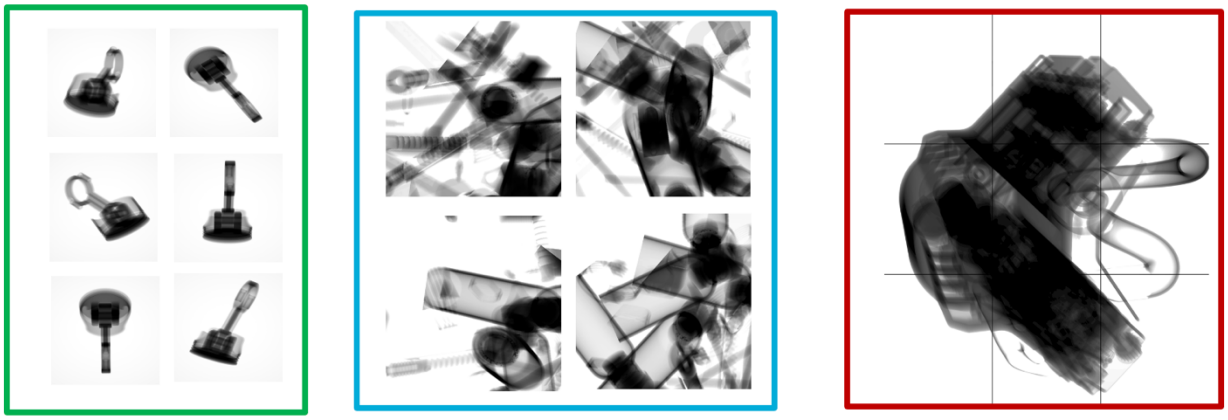

Figure 2 – Left: examples of pistons (analog design component of interest) imaged from 3072 orientations. Middle: randomly composed non-sensitive background scenes with everyday items for training. Right: the engine (analog sensitive context) for testing, where single panels (indicated by lines) were used for testing.

d) Synthetic Threat Insertion

Synthetically inserting items into radiographs is a common technique to create annotated radiograph datasets for object detection algorithms [3]. In contrast to photographs in which non-transparent items simply cover each other, transparent items multiplicatively combine. Pixel intensity on a detector is proportional to the x-ray intensity:

$$I = A\phi + B. \tag{3}$$

Using equations 2 and 3, in the case of multiple overlapping items, for example a background and a foreground object, the total intensity is:

$$I_{\text{total}} = A\phi_i e^{-\mu_{\text{background}}*d} e^{-\mu_{\text{foreground}}*d} + B. \quad (4)$$

In practice, imaging systems typically transform images for ease of viewing by a human inspector, and as a result the coefficients A and B are not known. If the additive offset is ignored, the total pixel intensity is proportional to the product of the intensities of the foreground and background if they would be imaged separately, $I_{\text{total}} \propto I_{\text{background}} I_{\text{foreground}}$. As a result, if there is a foreground object and a background which are imaged with roughly the same exposure settings, and they each span pixel values of 0-255, they can be combined:

$$I_{\text{total}} = \frac{I_{\text{background}} \times I_{\text{foreground}}}{255} \quad (5)$$

Effectively, the whiteness of the pixel becomes its transparency. In practice, the foreground needs to be lightened so that the background is white. Figure 3 shows this process of multiplicative insertion. A bounding box annotation can easily be generated from the smallest box that encloses non-white pixels in the foreground image (3a).

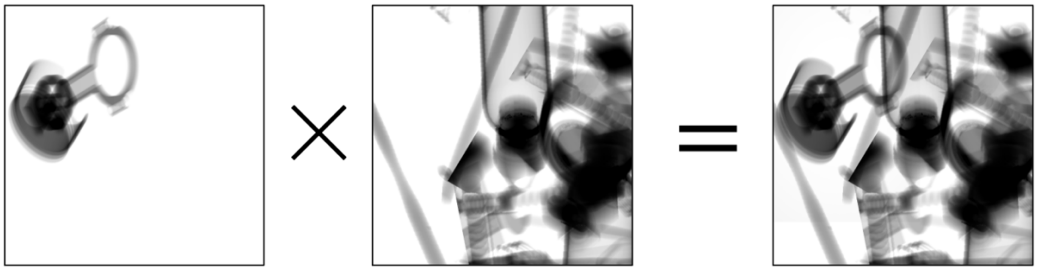

(a) (b) (c)

Figure 3 – Multiplicatively inserting a component into a background. The component, or foreground, is shown in (a) and inserted into the non-sensitive background (b) to produce image (c), which is optionally annotated using the smallest bounding box surrounding non-white pixels in (a).

To further augment the training dataset, we vary the magnification of the foreground object to a fraction of the background image size, between 0.25 +/- 0.05. We also vary the brightness by randomly multiplying by an adjustment factor between 0.85-1.25 and enforcing a maximum pixel value of 255. Finally, to ensure that the training examples are sufficiently challenging, we require that the foreground be inserted with a fraction of occluded pixels within 0.1-0.7, where an occluded pixel is defined as one in the foreground overlapping with a pixel in the background that is below a threshold of 70 (with white being 255).

e) Object Detection

As trust between treaty partners is paramount, we use an object detection algorithm rather than a simple object classifier, to be able to view the determinations that the model makes. Object detection algorithms are trained on annotated data and predict bounding boxes around items in images. However, as our goal is to simply classify presence or absence of components, we report classifier metrics.

We use the YOLO-v5 [4] algorithm to identify presence or absence of pistons, performing transfer learning using a Yolov5m model pre-trained on the COCO data set [5], trained to convergence in 100 epochs using a stochastic gradient descent optimizer.

In the test set and what would be expected in a real-world scenario, the car engine data does not have ground truth labels. Thus, traditional object detection metrics such as mean average precision (mAP) were not applied when evaluating on the training data. Instead, we are using the machine learning classification approach for determining precision and recall.

We report classification results using precision (P) and recall (R), defined in terms of true positive (TP), false positive (FP), and false negative (FN) determinations. Positives are reported with a confidence score cutoff of 0.4.

$$P = \frac{TP}{FP+TP} \tag{6}$$

$$R = \frac{TP}{TP+FN} \tag{7}$$

3) Results

Figure 4 shows several qualitative results of performing inference on the car engine test cases. As seen, the model can correctly predict the presence of the piston within the car engine even though it was not trained with examples of the piston in this context. Additionally, the model was only trained with one example of a piston, and it is able to identify multiple pistons within the car engine. Interestingly, the model seems to have learned the features of the piston head more than the entire body of the piston. When performing inference, it is seen by the positioning of the bounding boxes that the model puts more emphasis on the piston head.

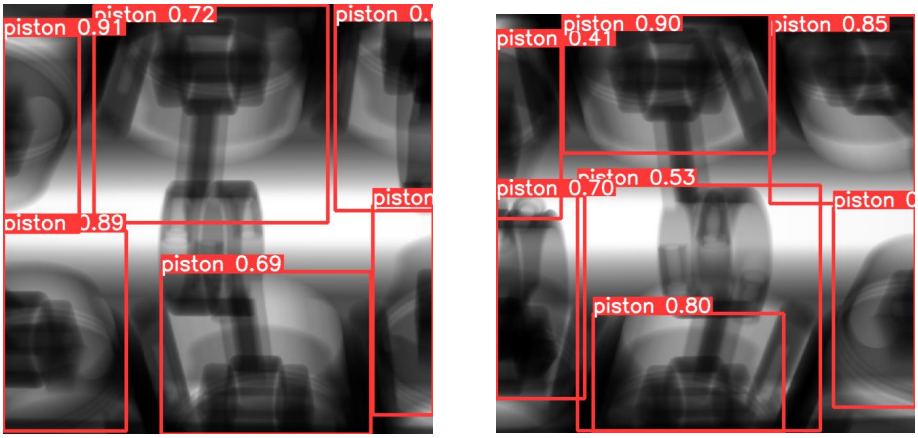

Figure 4 – Examples of object detection results YOLO model. The top left and right panels are cases where multiple pistons were present; whereas, the bottom two panels are single examples.

Table 1 shows the results for precision and recall from this analysis. The model is correctly predicting the presence of a piston 61% of the time while also correctly not predicting on radiographs that do not contain pistons 67% of the time. These results indicate the model is learning features of the piston that help better inform the prediction of presence or absence.

Precision	Recall
0.61	0.67

4) Discussion

We have demonstrated the feasibility of detecting a design component in a sensitive radiograph by training a deep learning-based object detection model on random, non-sensitive backgrounds with design components of interest synthetically inserted into them. These results advance a potential method for non-nuclear component verification in future arms control agreements, in which treaty partners agree upon shared components to identify behind an information barrier.

To expand upon this preliminary study, we will investigate methods of improving object detection performance in challenging, cluttered images whose elements are transparent. Object detection models are not specifically designed for inspecting transparent items, and as such, de-occlusion methods need to be developed. Furthermore, we will investigate how to better match the non-sensitive backgrounds to the characteristics of the test case, including how to transfer detector characteristics.

5) Acknowledgements

This article has been authored by an employee of National Technology & Engineering Solutions of Sandia, LLC under Contract No. DE-NA0003525 with the U.S. Department of Energy (DOE). The employee owns all right, title and interest in and to the article and is solely responsible for its contents. The United States Government retains and the publisher, by accepting the article for publication, acknowledges that the United States Government retains a non-exclusive, paid-up, irrevocable, world-wide license to publish or reproduce the published form of this article or allow others to do so, for United States Government purposes. The DOE will provide public access to these results of federally sponsored research in accordance with the DOE Public Access Plan https://www.energy.gov/downloads/doe-public-access-plan.

We thank Melinda Sweany, Kyle Polack, Jon Balajthy, Tom Weber, Eduardo Padilla, and Peter Marleau for their feedback.

7) References

[1] C. W. W. Charles Q. Little, Thomas M. Weber, Maikael A. Thomas, J. Derek Tucker, "Radiography Behind an Information Barrier for Warhead Verification," SAND2017-13465, 2017.

[2] C. W. W. Charles Q. Little, Thomas M. Weber, David K. Novick, "Processing Radiation Images Behind an Information Barrier for Automatic Warhead Authentication," Sandia National Laboratories, 2015.

[3] D. Mery, "Computer vision for X-Ray testing," *Switzerland: Springer International Publishing,* vol. 10, pp. 978-3, 2015.

[4] G. Jocher, "yolov5: v3.1," ed: Zenodo, 2020.

[5] T.-Y. Lin *et al.*, "Microsoft coco: Common objects in context," in *Computer Vision–ECCV 2014: 13th European Conference, Zurich, Switzerland, September 6-12, 2014, Proceedings, Part V 13*, 2014: Springer, pp. 740-755.